Volume 553, 20 November 2012 ISSN 0009-2614

ELSEVIER

CHEMICAL
PHYSICS
LETTERS

Frontier research in molecular sciences, materials and biological systems

FROM BALÁZS HAJGATÓ and MICHAEL S. DELEUZE, PAGES 6–10, IN THIS ISSUE.

www.elsevier.com/locate/cplett

Chemical Physics Letters 553 (2012) 21–25

Contents lists available at SciVerse ScienceDirect

Chemical Physics Letters

journal homepage: www.elsevier.com/locate/cplett

Raman study of the pressure-induced phase transitions in the molecular donor–acceptor complex $\{Pt(dbdtc)_2\}C_{60}$

K.P. Meletov [a],*, D.V. Konarev [b]

[a] Institute of Solid State Physics RAS, Chernogolovka, Moscow Region 142432, Russia
[b] Institute of Problems of Chemical Physics RAS, Chernogolovka, Moscow Region 142432, Russia

ARTICLE INFO

Article history:
Received 27 June 2012
In final form 21 September 2012
Available online 4 October 2012

ABSTRACT

Raman spectra of the molecular donor–acceptor complex $\{Pt(dbdtc)_2\}C_{60}$ (C_{60} fullerene with platinum dibenzyldithiocarbamate) were measured as a function of pressure up to 8 GPa. In the low pressure regime ($P < 0.5$ GPa), the phonon modes related to the C_{60} molecule split and soften, indicating the formation of intercage covalent bonds. Additional splitting of Raman modes is observed at ~2.5 GPa and is attributed to the formation of a polymeric network. The high-pressure phase remains stable upon pressure decrease, however at ~0.5 GPa the material transforms to a new phase characterized by a Raman spectrum which is quite different from those of the known polymers of C_{60}.

1. Introduction

Donor–acceptor complexes of C_{60} fullerene have been studied extensively with respect to their structural, optical, electrical and magnetic properties [1]. Fullerene complexes were synthesized with different classes of donor molecules, such as aromatic hydrocarbons, tetrathiafulvalenes, amines, metalloporphyrins, metallocenes and others [2]. Different organic donors form a wide family of compounds with fullerene, which have neutral as well as ionic ground states. The behavior of the donor–acceptor fullerene complexes at high pressure is of great interest due to the possibility of formation of polymeric networks between the fullerene molecules and/or the pressure-induced charge-transfer from the organic donor to the fullerene acceptor in the case of neutral ground state. At high pressure, the decrease of the interfullerene distances in the donor–acceptor complexes could cause the creation of covalent intercage bonds in directions with relatively short intermolecular distances. On the other hand, the overlap of the highest occupied molecular orbital (HOMO) of the molecular donor and the lowest unoccupied molecular orbital (LUMO) of the fullerene acceptor increases at high pressure making the charge transfer more favorable, particularly in the case where the molecular complex at ambient conditions is rather close to ionic. It is known that C_{60} molecules form linear chains in the co-crystallate of C_{60} with *p*-bromocalix(4)arene propyl ether after the treatment for 30 min at 200 °C under a pressure of 5 GPa [3]. The X-ray diffraction study of the ionic ground state donor–acceptor complexes of C_{60} has revealed the formation of the fullerene $(C_{120})^{2-}$ dimers bonded by one or two single bonds [4,5]. Raman spectra of the molecular donor–acceptor complex $C_{10}H_{12}Se_4{\cdot}C_{60}{\cdot}(CS_2)_2$ ($C_{10}H_{12}Se_4$ is tetramethyltetraselenofulvalene) at high-pressure show an irreversible phase transition at 5 GPa accompanied by the splitting and softening of the fullerene phonon modes [6]. Recently, the high-pressure study of the fullerene complex $C_{60}\{Fe(C_5H_5)_2\}_2$, ($Fe(C_5H_5)_2$ is ferrocene) has revealed the signs of the charge transfer accompanied by reversible polymerization of the fullerene sublattice at pressure ~5 GPa [7]. Moreover, the reversible changes in the Raman spectra of the molecular donor–acceptor complex $\{Ni(nPr_2dtc)_2\}(C_{60})_2$ observed in the pressure region of 0.5–2.5 GPa may be also associated with charge transfer and/or the formation of fullerene dimers [8].

The ability of C_{60} to form intercage covalent bonds is due to the existence of 30 unsaturated double C=C bonds in the fullerene molecule. The pristine C_{60} polymerizes under light illumination [9], alkali metal doping [10,11] and high-pressure/high-temperature treatment [12,13]. The intercage bonds are usually formed through four-membered rings by [2 + 2] cycloaddition reactions. This results in the symmetry lowering of the C_{60} molecule accompanied by the splitting and softening of phonon modes [9]. The most characteristic probe of the C_{60} polymer formation is the behavior of the $A_g(2)$ pentagonal pinch (PP) mode related to the in-phase stretching vibration, which involves tangential displacements of carbon atoms with a contraction of the pentagonal rings and an expansion of the hexagonal rings. The PP-mode frequency downshifts due to the continuous lowering of the intramolecular average bond stiffness as the number of intercage bonds per fullerene molecule increases.

In the present Letter, we report the Raman study of the pressure-induced transitions in the molecular donor–acceptor complex $\{Pt(dbdtc)_2\}C_{60}$ at pressures up to 8 GPa. In the low pressure regime, $P < 0.5$ GPa, the phonon modes of the C_{60} molecule split and soften, reflecting the transformation of the fullerene sublattice. At the pressure of ~2.5 GPa additional changes in the Raman

---

* Corresponding author. Fax: +7 49652 28160.
E-mail address: mele@issp.ac.ru (K.P. Meletov).

0009-2614/$ - see front matter © 2012 Elsevier B.V. All rights reserved.
http://dx.doi.org/10.1016/j.cplett.2012.09.050

spectrum occur, especially in the region of the PP-mode. These changes, most likely, may be associated with the formation of a polymeric network, the characteristic features of this spectrum are reminiscent of the corresponding features observed in the rhombohedral polymer of C_{60} at similar pressures. The high-pressure phase is stable upon pressure decrease down to $\sim$0.5 GPa, while at lower pressure it transforms to a phase characterized by a Raman spectrum which is different from those of known polymers of C_{60}. The final phase is stable after total release of pressure for at least a period of 2 weeks and does not change after annealing at 100 °C for 6 h. Nevertheless, the laser-induced heating at elevated laser powers tends to recover the initial Raman spectrum of the $\{Pt(dbdtc)_2\}C_{60}$ complex.

2. Experimental details

The $\{Pt(dbdtc)_2\}C_{60}\cdot(C_6H_5Cl)_{0.5}$ complex was synthesized by the evaporation of a solution containing fullerene C_{60} and platinum dibenzyldithiocarbamate in chlorobenzene [14]. As for the preparation of the solvent free $\{Pt(dbdtc)_2\}C_{60}$ phase, the synthetic procedure was modified. The hexagonal prisms of this complex were obtained by the slow diffusion of hexane solution of $Pt(dbdtc)_2$ (16 mg is dissolved in 25 mL of hexane) into a benzene solution of C_{60} (20 mg is dissolved in 20 mL of benzene), the black-brown crystals grown in this way were washed with hexane (yield 64%).

The X-ray data of the $\{Pt(dbdtc)_2\}C_{60}$ complex show that it adopts the monoclinic structure (space group $P2_1/c$). The parameters of the unit cell are $a = 15.957(5)$, $b = 17.241(5)$, $c = 10.018(5)$ Å, $\beta = 92.356(5)^\circ$, and $V = 2753.7(5)$ Å^3. The compound has a composition of $\{Pt(dbdtc)_2\}C_{60}$ and possesses a layered structure. Close-packed fullerene layers have an arrangement of the C_{60} molecules in a nearly hexagonal way. Six C_{60} molecules surround each C_{60} molecule in the layer with the shortest distances between the centers of fullerene molecules being 9.97 (four neighbors) and 10.02 Å (two neighbors). Since the 9.97 and 10.02 Å distances are shorter than the van der Waals (vdW) diameter of C_{60} molecule multiple vdW C…C contacts are formed between fullerenes of 3.20–3.48 Å length. No C–C bonds were found between fullerenes and therefore the fullerene sublattice of the complex is monomeric at ambient pressure. Fullerene layers alternate with the $Pt(dbdtc)_2$ molecular donor layers. The $Pt(dbdtc)_2$ molecules are arranged to the fullerenes by benzyl substituents to form several $C(Pt(dbdtc)_2)\ldots C(C_{60})$ vdW contacts in the 3.24–3.36 Å range. No covalent or coordination bonds were found between $Pt(dbdtc)_2$ and C_{60}. The arrangement of the fullerene and platinum dibenzyldithiocarbamate molecules in the plain perpendicular to the *a*-axis of the primitive cell is shown in the inset of Figure 1b [15].

Raman spectra from well-facetted crystals of the $\{Pt(dbdtc)_2\}C_{60}$ complex of $\sim$50 μm in diameter were recorded *in-situ* in the backscattering geometry using a micro-Raman setup that comprised of an Acton SpectraPro-2500i spectrograph and a Pixis2K CCD detector system cooled down to −70 °C. The 532 nm line of CW diode pumped YAG laser was focused on the sample by means of an Olympus 50× objective in a spot of $\sim$10 μm diameter due to slight defocusing. The laser line was suppressed by a super-notch filter with an optical density of OD = 6 and $\sim$160 cm^{-1} bandwidth, while the beam intensity before the diamond-anvil cell (DAC) was $\sim$0.7 mW. Measurements of the Raman spectra at high pressure were carried out using a DAC of Mao-Bell type. The 4:1 methanol/ethanol mixture was used as the pressure transmitting medium and the ruby fluorescence technique was used for pressure calibration [16].

3. Results and discussion

The Raman spectra of various specimens of the $\{Pt(dbdtc)_2\}C_{60}$ complex, recorded at ambient conditions and different laser power in the energy region of 150–1800 cm^{-1}, are illustrated in Figure 1. The phonon modes associated to the C_{60} molecule dominate the spectra (Figure 1a, laser power 0.16 mW), whereas the modes of the molecular donor are absent, probably due to their relatively small Raman scattering cross-section. On the contrary, the IR-absorption spectra of the $\{Pt(dbdtc)_2\}C_{60}$ complex contain both the fullerene C_{60} and $Pt(dbdtc)_2$ vibration modes (not shown here). In the Raman spectrum illustrated in Figure 1b, recorded at the same site of the sample with reduced laser power (0.07 mW), several new split components of the $A_g(1)$, $H_g(1)$ and $A_g(2)$ modes appear. Finally, the Raman spectrum of another sample, recorded also at the same laser power of 0.07 mW, clearly demonstrates the splitting of the degenerate H_g modes as well as of the non-degenerate A_g modes (Figure 1c). The vertical dotted lines in Figure 1 denote the Raman mode frequencies of the C_{60} monomer while the arrows mark the new Raman peaks. The new peaks in Figure 1b and c are related to the C_{60} dimer [17], but the Raman modes of the C_{60} monomer are also present in the spectra. Thus, it becomes evident that the $\{Pt(dbdtc)_2\}C_{60}$ complex synthesized in this Letter contains both monomers and dimers of C_{60}. The presence of dimers at ambient conditions can be explained taking into account the relatively short distances between the C_{60} molecules that may become even smaller due to local strains. The Raman modes of the C_{60} dimers disappear at elevated laser excitation powers most likely due to the laser heating which induces an expansion of the structure and the removal of strains.

The Raman spectra in the frequency region of 150–1800 cm^{-1} of the $\{Pt(dbdtc)_2\}C_{60}$ complex, at various pressures up to 8 GPa, are illustrated in Figure 2. The left and right panels in Figure 2 show the spectra recorded upon pressure increase and decrease, respectively. The spectral region around the strong triply degenerate T_{2g} mode of diamond, appearing at 1332 cm^{-1} at ambient pressure [18], is excluded. The background has been subtracted from the experimental spectra. The initial Raman spectrum, after cell loading, at pressure 0.01 GPa is similar to the spectrum of Figure 1c that indicates the presence of C_{60} dimers in the sample. As the pressure increases, the majority of Raman peaks shift to higher energies, however some modes exhibit negative pressure shift. In addition, the $A_g(1)$, $A_g(2)$ and $H_g(8)$ modes soften in the low pressure region, while at higher pressure their behavior is reversed exhibiting a positive pressure shift. The splitting and softening of the Raman modes, as well as the redistribution of their intensity in the pressure region up to 0.5 GPa are the unambiguous signs of the pressure-induced transformation in the fullerene sublattice. The transformation shown in the Raman spectrum under pressure is similar to that observed in the pristine C_{60} which undergoes polymerization under high temperature/high pressure treatment [12,13]. It is interesting to note, that the non-degenerate PP-mode splits into three components of comparable intensity. The pressure response of the phonon modes after further increase of pressure is smooth up to 2.5 GPa where an additional mode splitting and intensity redistribution takes place. The most important change near 2.5 GPa is the appearance of a fourth component of the PP-mode with a frequency of $\sim$1414 cm^{-1}. The relative intensity of this component increases rapidly with pressure and finally this new peak dominates the spectrum. Afterward, the pressure response of the Raman spectra is smooth and does not show any singularities up to the highest pressure attained in our experiments (8 GPa). It is interesting that the Raman spectrum of the $\{Pt(dbdtc)_2\}C_{60}$ complex for $P > 2.5$ GPa is reminiscent to that of the rhombohedral crystalline polymer of C_{60} at similar pressures; the resemblance is more pronounced in the energy region of the PP-mode [19,20].

The Raman spectra of the $\{Pt(dbdtc)_2\}C_{60}$ complex, recorded upon pressure decrease (right panel in Figure 2), demonstrate a smooth evolution without any singularities down to $\sim$0.5 GPa,

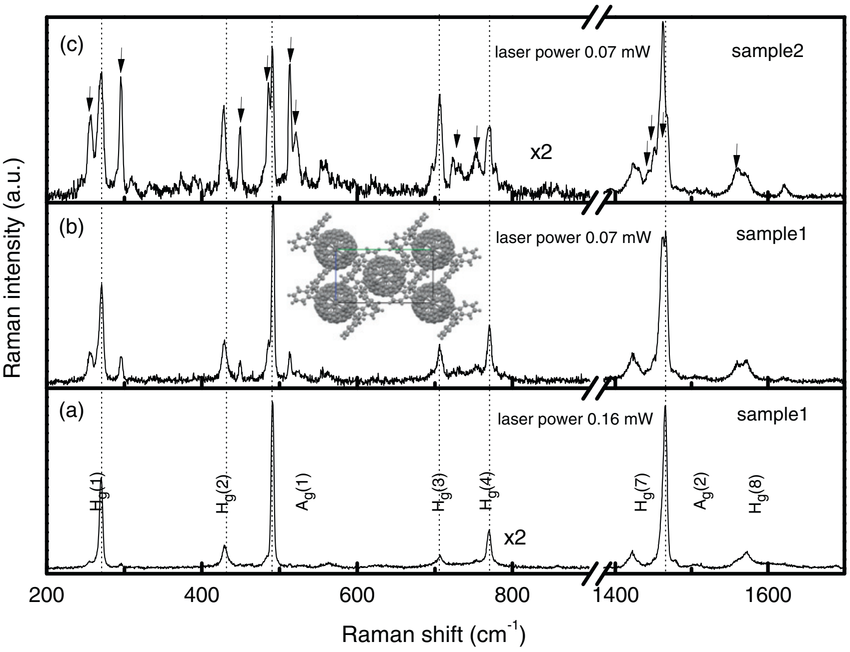

Figure 1. Raman spectra of various specimens of the $\{Pt(dbdtc)_2\}C_{60}$ complex recorded at ambient conditions and for different laser excitation power in the energy region of 150–1800 cm^{-1}. Arrows mark the split modes. The inset depicts the arrangement of fullerene and platinum dibenzyldithiocarbamate molecules in the plain perpendicular to the a-axis of the primitive cell.

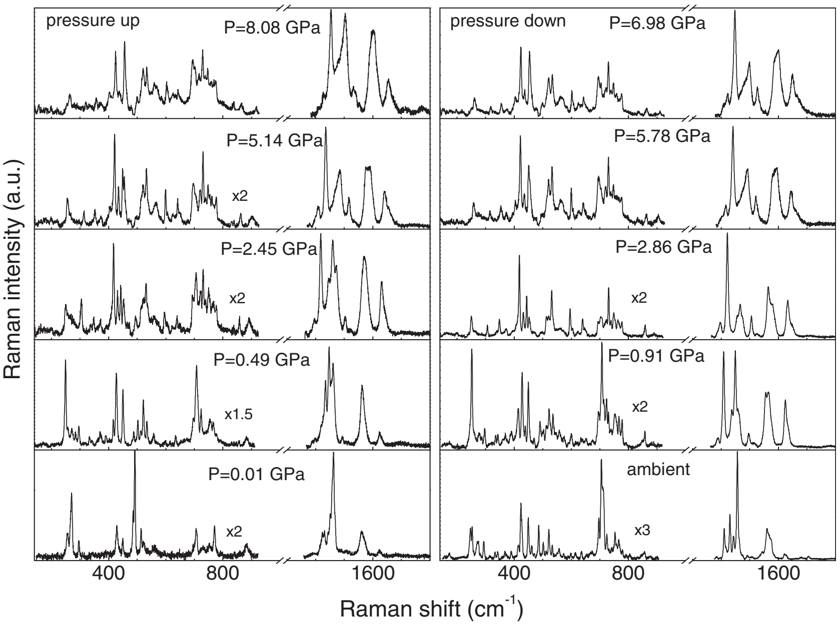

Figure 2. Raman spectra in the frequency region of 150–1800 cm^{-1} of the $\{Pt(dbdtc)_2\}C_{60}$ complex as a function of pressure up to 8 GPa. Left (right) panel depicts spectra recorded for increasing (decreasing) pressure.

where a new transformation takes place. The first indication of the incoming transformation is observed in the Raman spectrum of the complex at $P = 0.91$ GPa, where the relative intensity of the split component of the PP-mode near 1408 cm^{-1} decreases noticeably. Finally, after total pressure release, the Raman spectrum of the $\{Pt(dbdtc)_2\}C_{60}$ complex (bottom spectrum in the right panel of Figure 2) differs from that recorded at the initial pressure after cell loading; the difference concerns to both the number of the split modes as well as the intensity distribution between them. Therefore, the transformations observed under high pressure are not reversible and the Raman spectrum of the recovered material indicates a polymerized fullerene sublattice.

The pressure dependence up to 8 GPa of the Raman peak frequencies of the $\{Pt(dbdtc)_2\}C_{60}$ complex is shown in Figure 3. The left panel illustrates the pressure evolution of the Raman peaks in the frequency region of 240–545 cm^{-1}, while the right panel in the region of 1390–1695 cm^{-1}. Open (close) symbols represent data for increasing (decreasing) pressure. The pressure shift of almost all modes is positive except that of the $H_g(3)$ and $H_g(4)$ modes that show a negative pressure shift (not shown in Figure 3). The

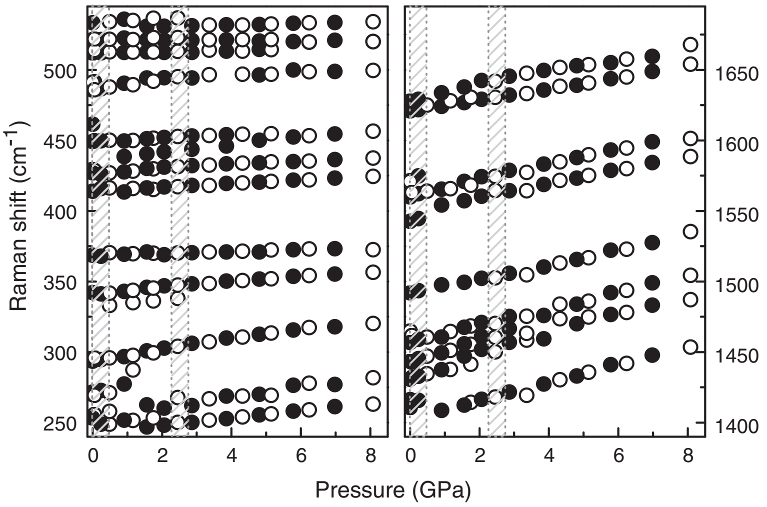

Figure 3. Pressure dependence of the Raman mode frequencies of {Pt(dbdtc)$_2$}C$_{60}$ in the pressure region up to 8 GPa. Left (right) panel depicts the phonon modes in the energy region of 240–545 cm^{-1} (1390–1695 cm^{-1}). Open (close) symbols correspond to data recorded upon increasing (decreasing) pressure. Shaded areas indicate the pressure regions where the phase transitions take place.

pressure coefficients $d\omega/dP$ vary between -1.6 and 6.4 cm^{-1}/GPa for the different Raman modes. Shaded areas indicate the pressure regions near 0.5 and 2.5 GPa where the changes in the pressure behavior of Raman modes take place. These changes are associated with the softening of the A$_g$(1), A$_g$(2) and H$_g$(8) modes in the initial pressure region ($P < 0.5$ GPa) and the splitting of Raman modes near 0.5 and 2.5 GPa. We believe that the changes in the Raman spectra are due to the induced phase transitions related to the polymerization of the fullerene sublattice. The data obtained upon pressure decrease differ from those recorded for pressure increase, revealing that the phase transitions are irreversible. More precisely, the high-pressure phase persists down to ~0.5 GPa, where the transformation, probably to another polymeric network, is taking place. In contrast to the initial monomer state, the final state of the {Pt(dbdtc)$_2$}C$_{60}$ complex is polymerized one.

The polymerized {Pt(dbdtc)$_2$}C$_{60}$ complex after pressure release is rather stable; the Raman spectrum of the recovered material remains practically unchanged 2 weeks after pressure release even after heat treatment. Generally, the C$_{60}$ polymers are not stable at elevated temperature; heating to 260 °C results in the recovery of the C$_{60}$ monomer phase [21–23]. Figure 4 shows the Raman spectra of the {Pt(dbdtc)$_2$}C$_{60}$ complex in the energy region of the PP-mode recorded under various conditions. The spectrum in Figure 4a refers to the initial monomer state of the {Pt(dbdtc)$_2$}C$_{60}$. The spectrum in Figure 4b was recorded 2 weeks later after pressure release and does not change after heat treatment at 100 °C for 6 h. Finally, the spectrum in Figure 4c was recorded at higher laser power which causes the overheating of the sample within the laser spot [24]. The laser-induced heating changes drastically the Raman spectrum: the intensity of the peak near 1456 cm^{-1} decreases and two new peaks at ~1462 and ~1467 cm^{-1} appear, corresponding to the dimer and monomer of C$_{60}$, respectively. In addition, the peak at 1410 cm^{-1} is suppressed while a new weak peak near 1451 cm^{-1} appears. These changes clearly indicate the destruction of the intercage bonds and the fragmentation of the polymeric network. Further increase of the laser intensity leads to complete decomposition of the polymeric network so that the peak at ~1467 cm^{-1} dominates the Raman spectrum. This latter spectrum (not shown) is dominated by strong luminescence background and a significant decrease of the signal-to-noise ratio.

In polymeric C$_{60}$ networks the softening of the PP-mode increases with the number of the intermolecular links, the minimum softening being that of ~5 cm^{-1} for the C$_{60}$ dimers (two sp^3-like coordinated carbon atoms per fullerene molecule) [17]. This softening in linear polymeric chains is 12 cm^{-1} (four sp^3-like coordinated carbon atoms per fullerene molecule) [25]. In the planar tetragonal and rhombohedral crystalline polymers of C$_{60}$ the softening is 20 and 60 cm^{-1} respectively (8 and 12 sp^3-like coordinated carbon atoms per fullerene molecule, respectively) [26]. The inset in Figure 4c illustrates the dependence of the A$_g$(2) Raman mode frequency on the number of the sp^3-like coordinated carbon atoms per fullerene molecule for the various polymeric networks of C$_{60}$ (open circles). This dependence has been established by detailed X-ray, IR and Raman studies of the crystal structure and phonon spectra of the crystalline polymers of C$_{60}$ [12,13,25,26]. The closed circles show the frequencies of the split components of the PP-mode in the Raman spectrum of the {Pt(dbdtc)$_2$}C$_{60}$ complex after pressure release, as well as for the peaks appearing when the sample is subject to annealing by the higher laser excitation power (marked by arrows in Figure 4). The excellent agreement between these data means that the polymeric network in the {Pt(dbdtc)$_2$}-C$_{60}$ after pressure release is rather complicated and involves C$_{60}$ cages with various number of the sp^3-like coordinated carbon atoms per molecule. The narrow peaks and the rich structure of the spectra are indicative of an ordered crystalline structure. The number of peaks and the intensity distribution in the region of the PP-mode cannot be associated to only one of the known crystalline polymers of C$_{60}$ [12,13]. However, the frequencies of the split components of the PP-mode: 1456, 1444, 1430 and 1410 cm^{-1} are typical for fullerene molecules with 4, 8, 10 and 12 sp^3-like coordinated carbon atoms per cage, respectively, while their intensities should be related to their relative abundance in the particular structure. Taking into account the frequencies and intensities of the split components of the PP-mode, we can assume that the fullerene sublattice of the {Pt(dbdtc)$_2$}C$_{60}$ complex after pressure release forms partially conjugated linear polymeric chains. It is interesting to note, that Raman peaks at 1430 and 1451 cm^{-1}, related to C$_{60}$ molecules with 10 and 6 sp^3-like coordinated carbon atoms per molecule, respectively, have never been observed earlier in the crystalline polymers of C$_{60}$. Finally, we are planning to undertake an X-ray diffraction study at high pressure

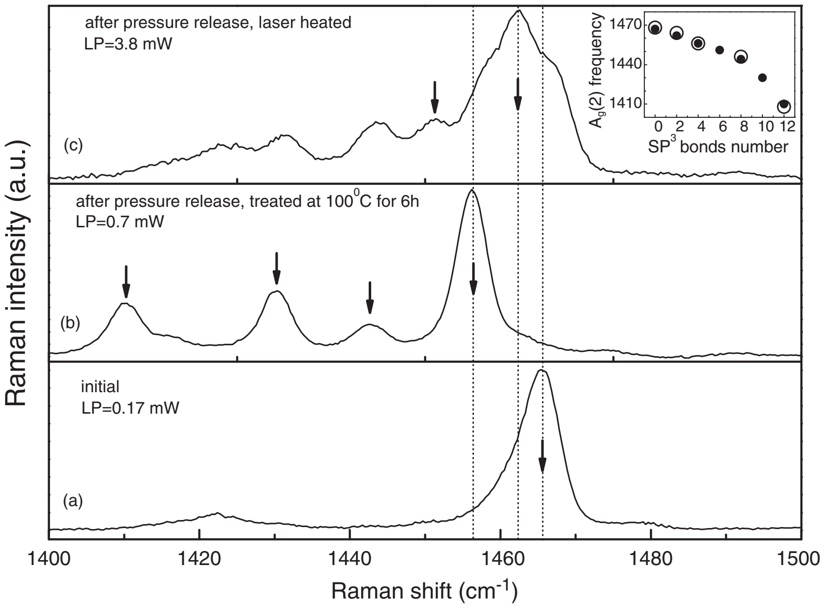

Figure 4. Raman spectra of the $\{Pt(dbdtc)_2\}C_{60}$ complex in the energy region of PP-mode recorded under various conditions of pressure application, excitation power and annealing. (a) Raman spectrum of the pristine $\{Pt(dbdtc)_2\}C_{60}$. (b) Raman spectrum of the complex after 2 weeks from the pressure release and treated at 100 °C for 6 h. (c) Raman spectrum of the recovered sample after laser heating. Inset: PP-mode frequency vs. number of sp^3-like coordinated carbon atoms per fullerene cage. Open circles: crystalline polymers of C_{60}. Closed circles: the split components of the PP-mode in the Raman spectrum of the $\{Pt(dbdtc)_2\}C_{60}$ after pressure release.

to clarify the structural aspects of the observed pressure-induced phase transitions.

Acknowledgements

The support by the Russian Foundation for Basic Research, Grant No. 11-02-00886, and RAS Presidium Program 'Physics of the extremely compressed matter' is greatly acknowledged.

References

[1] D.V. Konarev, S.S. Khasanov, D.V. Lopatin, V.V. Rodaev, R.N. Lyubovskaya, Russ. Chem. Bull. Int. Ed. 56 (2007) 2145.
[2] D.V. Konarev et al., J. Mat. Chem. (2000) 803.
[3] D. Sun, C.A. Reed, Chem. Commun. (2000) 2391.
[4] D.V. Konarev, S.S. Khasanov, G. Saito, A. Otsuka, Y. Yoshida, R.N. Lyubovskaya, J. Am. Chem. Soc. 125 (2003) 10074.
[5] D.V. Konarev, S.S. Khasanov, A. Otsuka, G. Saito, R.N. Lyubovskaya, J. Am. Chem. Soc. 128 (2006) 9292.
[6] K.P. Meletov et al., Chem. Phys. Lett. 281 (1997) 360.
[7] Wen Cui et al., J. Phys. Chem. B 116 (2012) 2643.
[8] K.P. Meletov, D.V. Konarev, Fullerenes, Nanotubes, Carbon Nanostruct. 20 (2012) 336.
[9] A.M. Rao et al., Science 259 (1993) 955.
[10] J. Winter, H. Kuzmany, Solid State Commun. 84 (1992) 935.
[11] P.W. Stephens et al., Nature 370 (1994) 636.
[12] Y. Iwasa et al., Science 264 (1994) 1570.
[13] M. Nunez-Regueiro, L. Marques, J.-L. Hodeau, O. Bethoux, M. Perroux, Phys. Rev. Lett. 74 (1995) 278.
[14] D.V. Konarev, A.Yu. Kovalevsky, A. Otsuka, G. Saito, R.N. Lyubovskaya, Inorg. Chem. 44 (2005) 9547.
[15] S.S. Khasanov, D.V. Konarev et al., in press.
[16] A. Jayaraman, Rev. Sci. Instrum. 57 (1986) 1013.
[17] S. Lebedkin, A. Gromov, S. Giesa, R. Gleiter, B. Renker, H. Rietschel, W. Krätschmer, Chem. Phys. Lett. 285 (1998) 210.
[18] S.A. Solin, A.K. Ramdas, Phys. Rev. B 1 (1970) 1687.
[19] K.P. Meletov, J. Arvanitidis, G.A. Kourouklis, Y. Iwasa, K. Prassides, Chem. Phys. Lett. 357 (2002) 307.
[20] K.P. Meletov, G.A. Kourouklis, J. Arvanitidis, K. Prassides, Y. Iwasa, Phys. Rev. B 68 (2003) 094103.
[21] Y. Iwasa, K. Tanoue, T. Mitani, T. Yagi, Phys. Rev. B 58 (1998) 16374.
[22] M.V. Korobov, V.M. Senyavin, A.G. Bogachev, E.B. Stukalin, V.A. Davydov, L.S. Kashevarova, et al., Chem. Phys. Lett. 381 (2003) 410.
[23] K.P. Meletov, J. Arvanitidis, D. Christofilos, G.A. Kourouklis, Y. Iwasa, S. Yamanaka, Carbon 48 (2010) 2974.
[24] K.P. Meletov, E. Liarokapis, J. Arvanitidis, K. Papagelis, D. Palles, G.A. Kourouklis, S. Ves, Chem. Phys. Lett. 290 (1998) 125.
[25] V.M. Senyavin et al., Chem. Phys. Lett. 313 (1999) 421.
[26] V.A. Davydov et al., Phys. Rev. B 61 (2000) 11936.